24th COBEM - 2017

24th ABCM International Congress of Mechanical Engineering
December 3-8, 2017, Curitiba, PR, Brazil

COBEM-2017-1910
DESIGN AND APPLICATION OF A STATIC $\mathcal{H}_\infty$ CONTROL FOR AN ACTIVE SUSPENSION SYSTEM

Diego Alves da Mata
Marina dos Santos Coimbra
Renan Lima Pereira
Universidade Federal de Itajubá - Campus Itabira. Rua Irmã Ivone Drumond, 200 - Distrito Industrial II - 35903 - 087, Itabira, Minas Gerais, Brasil
diegoadmata@gmail.com, marinascoimbra@hotmail.com, renan.lima@unifei.edu.br

Abstract. *In this work, a static $\mathcal{H}_\infty$ loop shaping controller design based on Linear Matrix Inequalities (LMIs) applied to an active suspension system is provided. Sufficient LMIs conditions for continuous-time systems are used in order to obtain a static $\mathcal{H}_\infty$ loop shaping controller that ensures the robust stability and performance for the closed-loop system. The procedure has two steps. First, the open-loop plant is shaped by pre (W_1) and post-compensators (W_2) to give a desired shape to the singular values of the open-loop frequency response. In the second step, the controller is then calculated in order to satisfy the $\mathcal{H}_\infty$ performance index. Differently from other works in the literature, the robust control formulation adopted in this study assumes that the active suspension system is subject to nonparametric uncertainties described by left coprime factorization and that the stabilizing controller is designed to maximize a measure of robustness, represented by an admissible upper bound. After finding the static $\mathcal{H}_\infty$ loop shaping controller, experiments were performed on the active suspension system manufactured by Quanser Consulting. The masses were varied and the results compared with the responses in open-loop. The experimental results showed that the static $\mathcal{H}_\infty$ loop shaping controller designed may be an advantageous alternative for the control of mechanical systems.*

Keywords: *Active suspension system, static $\mathcal{H}_\infty$ loop shaping controller, LMIs.*

1. INTRODUCTION

The irregularities on the roads may cause discomfort and even accidents. The straightforward manner used to mitigate the effects of road variations is the suspension. In a real situation, a suspension system is responsible for providing ride comfort, restricting the displacement between the vehicle body and the tire in an allowable workspace and preserving the contact forces between the road surface and the vehicle (Quanser, 2013). The suspension system can be divided into two categories: passive suspension - with only springs and shock absorbers - and active suspension - with actuators that use external power to attenuate the effects of the oscillations. Concerning application of active suspension systems, a mathematical model under analysis must be available to the designer. However, this adopted model provides only a simplified mathematical description of the phenomenon that represent it. In this sense, the problem arises when the same vehicle travels only with a driver or with all passengers and full of luggage causing a large difference in the total weight. In addition, other variations in the model can be given by tire calibration and disrepair of suspension components.

In order to circumvent these mismatches inherent in the active suspension's nominal model, a control design strategy to ensure stability and comfort is recommended. Different classes of compensation-type controllers can be considered to solve this problem. For instance, robust control techniques have been shown to be particularly interesting due to their capability of taking into account typical uncertainties. There are several robust control techniques employed to tolerate the mismatch between nominal model and real model as: full-order sliding mode (Fazzolari *et al.*, 2014) ; switched $\mathcal{H}_\infty$ control (Oliveira *et al.*, 2014a); $\mathcal{H}_\infty$ multiobjective (Oliveira *et al.*, 2014b) and others (Alves *et al.*, 2013) (Silva *et al.*, 2013). As a result, the $\mathcal{H}_\infty$ theory has been playing an important role to deal with this issue. Differently from other papers in the literature, a particular approach that has received increasing attention due to the reduced effort for practical controller implementations is the static $\mathcal{H}_\infty$ loop shaping controller method proposed in (Prempain and Postlethwaite, 2005; Pereira *et al.*, 2017a). This approach may lead to advantageous results over classical design methods. This is due mainly to the ease to accomplish trade-off in terms of performance requirements and robustness to uncertainties. Moreover, such approach aims at measuring a system's capacity to reject energy bounded disturbances.

In this context, the main contribution of this paper consists in the practical investigation of a static $\mathcal{H}_\infty$ loop shaping controller design applied to an active suspension system. The active suspension system used herein was produced by Quanser Consulting and its dynamics can be described by a fourth-order system composed by two masses and two springs,

which are independent storage elements, that represents a quarter-car model.

This paper is structured as follows. In the Section 2, the modeling of the Quanser's active suspension system is derived. Section 3 details the static $\mathcal{H}_\infty$ loop shaping control method for continuous-time systems. Section 4 presents the experimental results obtained. Finally, the conclusions are given in Section 5.

The notation used in this paper is: $\bullet$ is a symmetric block in a matrix, $\mathbb{R}^{n\times n}$ represents the set of real numbers $n \times m$ matrices, I_n is an identity matrix, $M > 0$ (or $M < 0$) means M is symmetric and positive (or negative) definite.

2. DESCRIPTION AND MODELING OF THE ACTIVE SUSPENSION SYSTEM

The active suspension system used here was produced by Quanser Consulting (Fig. 1) and its dynamics can be described by a proper system . The rotary movement of the electric motor CC1 is converted to linear. This movement simulates the variations on the road. The first platform represents the road. The second platform represents the wheel and tire that is considered a unsprung mass. The third platform represents the body of the vehicle that is considered a sprung mass. The electric motor CC2 is responsible for acting on the active suspension control and keep the third platform suspended. Two removable discs can be used to simulate the load. In addition, the system has two encoders to indicate in a joint way the positions of the three platforms.

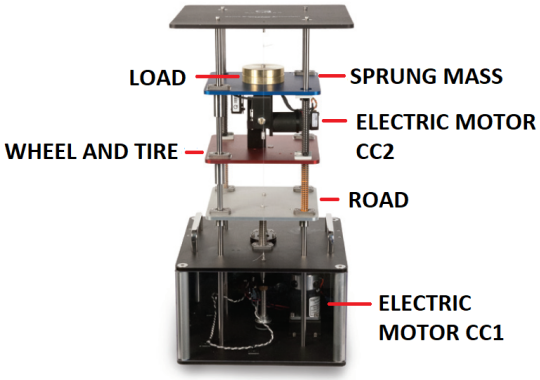

Figure 1. Quanser's Active suspension system (adapted from Quanser (2013)).

The active suspension system is a fourth-order system composed by two masses and two springs. The interactions of the system components is shown in Fig. 2.

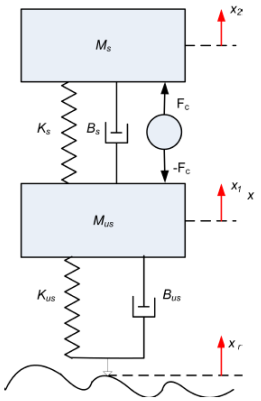

Figure 2. Spring-mass-damper system (adapted from Quanser (2013)).

The adopted model follows (Quanser, 2013) that uses the free-body diagram to obtain a nominal model. The inputs are the power of the electric motor $F_c(s)$ and the oscillations of the road x_r. The other variables are described in the Table 1. An analysis of the forces acting on each mass was made to find the equations that describe the system. The forces acting on M_s are presented from the free-body diagram (Fig. 3a). Considering the null initial conditions and gravity being g, the acceleration of M_s is given by

$$\ddot{x}_2 = -g + \frac{F_c}{M_s} + \frac{B_s\dot{x}_1}{Ms} - \frac{B_s\dot{x}_2}{M_s} + \frac{K_s x_1}{M_s} - \frac{K_s x_2}{M_s}. \tag{1}$$

Table 1. Constants used to describe the laboratory plant (adapted from Quanser (2013)).

Symbol	**Physical meaning**	**Value**
M_s	Mass of the vehicle body	$2.45[kg]$
M_{us}	Mass of wheel and tire	$1[kg]$
K_s	Const. of spring between M_s and M_{us}	$900[N/m]$
K_{us}	Const. of spring between M_{us} and road	$1250[N/m]$
B_s	Const. of bumper between M_s and M_{us}	$7.5[Nseg/m]$
B_{us}	Const. of bumper between M_{us} and road	$5[Nseg/m]$

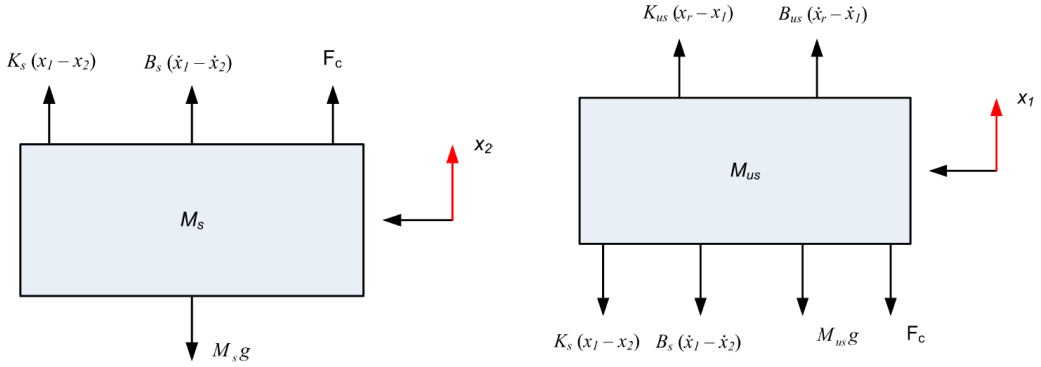

Figure 3. a) Free-body diagram for M_s (adapted from Quanser (2013)); b) Free-body diagram for M_{us} (adapted from Quanser (2013)).

Analogously, we can describe the forces acting on M_{us} from the free-body diagram (Fig. 3b). Thus, the acceleration of M_s is

$$\ddot{x}_1 = -g - \frac{F_c}{M_{us}} - \frac{(B_s + B_{us})\dot{x}_1}{M_{us}} + \frac{B_s\dot{x}_2}{M_{us}} + \frac{B_{us}\dot{x}_r}{M_{us}} - \frac{(K_{us} + K_s)x_1}{M_{us}} + \frac{K_s x_2}{M_{us}} + \frac{x_r Kus}{M_{us}}. \tag{2}$$

In this case, the gravity force changes only the equilibrium point without interfering with the dynamics. Adopting the following equilibrium points($x_1 = x_{eq1}$ and $x_2 = x_{eq2}$) and replacing such changes in Equations (1) and (2) is obtained

$$x_{eq1} = -\frac{g(M_s + M_{us})}{K_{us}}; \qquad x_{eq2} = -\frac{g(M_s K_{us} + K_s M_s + K_s M_{us})}{K_{us} K_s}. \tag{3}$$

In order to remove the force of gravity, the following substitutions are suggested:

$$x_1 = x_{1us} - \frac{g(M_s + M_{us})}{K_{us}}, x_2 = x_{2s} - \frac{M_s g}{K_s} - \frac{g(M_s + M_{us})}{K_{us}}, \dot{x}_1 = \dot{x}_{1us}, \ \ddot{x}_1 = \ddot{x}_{1us}, \ \dot{x}_2 = \dot{x}_{2s} \tag{4}$$

Now, rewriting the Equations (1) and (2), we have

$$M_{us}\ddot{x}_{1us} = -B_s\dot{x}_{1us} - B_{us}\dot{x}_{1us} - F_c + B_s\dot{x}_{2s} + B_{us}\dot{x}_r - (x_{1us} - x_{2s})K_s - (x_{1us} - x_r)K_{us} \tag{5}$$

$$M_s\ddot{x}_{2s} = B_s\dot{x}_{1us} + F_c - B_s\dot{x}_{2s} - (x_{2s} - x_{1us})K_s. \tag{6}$$

Using the state-space realization,

$$G := \begin{cases} \dot{x}(t) = A_0 x(t) + B_0 u(t) \\ y(t) = C_0 x(t) + D_0 u(t) \end{cases} \tag{7}$$

where the states, inputs and outputs are represented by

$$x(t) = \begin{pmatrix} x_{2s} - x_{1us} \\ \dot{x}_{2s} \\ x_{1us} - x_r \\ \dot{x}_{1us} \end{pmatrix}, \quad u(t) = \begin{pmatrix} \dot{x}_r \\ F_c \end{pmatrix} \text{ and } \quad y(t) = \begin{pmatrix} x_{2s} - x_{1us} \\ \ddot{x}_{2s} \end{pmatrix}.$$

We can determine the matrices A_0, B_0, C_0, and D_0 that compose the state-space representation of the system G

$$A_0 = \begin{pmatrix} 0 & 1 & 0 & -1 \\ -\frac{K_s}{M_s} & -\frac{B_s}{M_s} & 0 & \frac{B_s}{M_s} \\ 0 & 0 & 0 & 1 \\ \frac{K_s}{M_{us}} & \frac{B_s}{M_{us}} & -\frac{K_{us}}{M_{us}} & -\frac{B_s+B_{us}}{M_{us}} \end{pmatrix}, \quad B_0 = \begin{pmatrix} 0 & 0 \\ 0 & \frac{1}{M_s} \\ -1 & 0 \\ \frac{B_{us}}{M_{us}} & -\frac{1}{M_{us}} \end{pmatrix}, \tag{8}$$

$$C_0 = \begin{pmatrix} 1 & 0 & 0 & 0 \\ -\frac{K_s}{M_s} & -\frac{B_s}{M_s} & 0 & \frac{B_s}{M_s} \end{pmatrix}, \quad D_0 = \begin{pmatrix} 0 & 0 \\ 0 & \frac{1}{M_s} \end{pmatrix}. \tag{9}$$

Despite of the active suspension system be MIMO (Multi-Input-Multi-Output), it was considered only the relation between the MOTOR CC 2 given by current input $I_{cc}(s)$ and acceleration of the vehicle $\ddot{x}_{2s} = a_{2s}$. Thus, the nominal model used is

$$\frac{A_{2s}(s)}{I_{cc}(s)} = \frac{0.047s^4 + 0.234s^3 + 58.67s^2}{s^4 + 15.56s^3 + 2533s^2 + 5663s + 460000} \tag{10}$$

Moreover, it worth to mentioning that the relation between the electric motor force $F_c(s)$ and the applied current $I_{cc}(s)$ is $0.115[N.m] = 1[A]$.

3. STATIC $\mathcal{H}_\infty$ LOOP SHAPING CONTROL METHOD FOR CONTINUOUS-TIME SYSTEMS

Consider a proper stabilizable and detectable system G_s of order n and m inputs,

$$G_s = \left[\begin{array}{c|c} A & B \\ \hline C & D \end{array}\right] \tag{11}$$

with $A \in \mathbb{R}^{n\times n}$, $B \in \mathbb{R}^{n\times m}$, $C \in \mathbb{R}^{p\times n}$ e $D \in \mathbb{R}^{p\times m}$. In this case, G_s is shaped with pre- and post- compensators ($G_s = W_2GW_1$) where G is nominal system. Following the (McFarlane and Glover, 1992) procedure, G_s can be represented from a left coprime factorization $G_s = \tilde{M}^{-1}\tilde{N}$, with

$$\left[\begin{array}{c|cc} \tilde{M}, \tilde{N} \end{array}\right] = \left[\begin{array}{c|cc} A+LC & B+LD & L \\ \hline E^{-1/2}C & E^{-1/2}D & E^{-1/2} \end{array}\right] \tag{12}$$

where $L = -(BD^T + ZC^T)E^{-1}$, $E = (I + DD^T)$ and the matrix $Z = Z^T > 0$ is the unique solution for algebraic Riccati equation (ARE),

$$(A - BF^{-1}D^TC)Z + Z(A - BF^{-1}D^TC)^T - ZC^TE^{-1}CZ + BF^{-1}B^T = 0 \tag{13}$$

with $F = I + D^TD$.

In this sense, the generalized system P can be described as (McFarlane and Glover, 1992),

$$\left[\begin{array}{c} \dot{x}(t) \\ \hline z(t) \\ y(t) \end{array}\right] = P \left[\begin{array}{c} x(t) \\ \hline w(t) \\ u(t) \end{array}\right] \tag{14}$$

with

$$P = \left[\begin{array}{c|c|c} A & -LE^{1/2} & B \\ \hline 0 & 0 & I_m \\ C & E^{1/2} & D \\ \hline C & E^{1/2} & D \end{array}\right] \tag{15}$$

where $x(t) \in \mathbb{R}^n$ is the vector of states, $u(t) \in \mathbb{R}^m$ is the control input, $w(t) \in \mathbb{R}^q$ is the exogenous input, $z(t) \in \mathbb{R}^v$ is the controlled output and $y(t) \in \mathbb{R}^p$ is the measured output. Now, adding nonparametric uncertainties ΔN and ΔM in coprime factors such that $\left\| \left[\begin{array}{cc} \Delta N & \Delta M \end{array}\right] \right\|_\infty \leq 1/\gamma$, the perturbed shaped plant may be defined as

$$G_s(\Delta) = (M + \Delta M)^{-1}(N + \Delta N). \tag{16}$$

Then, the $\mathcal{H}_\infty$ loop shaping control problem (Fig. 4) consists in determining a gain K that stabilizes the closed-loop system satisfying $\|T_{zw}\|_\infty \leq \gamma$,

$$\left\| \left[\begin{array}{c} K \\ I \end{array}\right] (I - G_sK)^{-1}\tilde{M}^{-1} \right\|_\infty < \frac{1}{\varepsilon} = \gamma \tag{17}$$

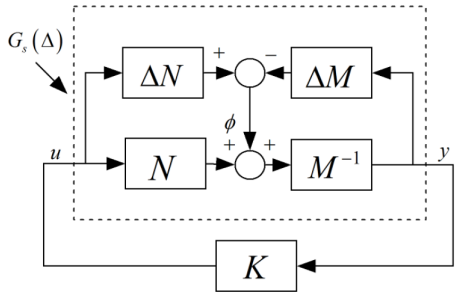

Figure 4. Closed-loop system for $\mathcal{H}_\infty$ loop shaping control problem.

where ε is an upper bound for nonparametric uncertainties and γ of the $\mathcal{H}_\infty$-norm .

Differently from the method proposed by (McFarlane and Glover, 1992), where the $\mathcal{H}_\infty$ controller K has high order, in this paper is used the procedure proposed by (Prempain and Postlethwaite, 2005), by means of the sufficient LMI conditions (19) and (20), which a static $\mathcal{H}_\infty$ loop shaping controller can be obtained.

Theorem 1 ((Prempain and Postlethwaite, 2005)) *From the gain $L = -(BD^T + ZC^T)E^{-1}$, there is a static controller $\mathcal{H}_\infty$ loop shaping K that satisfies,*

$$\left\| \begin{bmatrix} K \\ I \end{bmatrix} (I - G_s K)^{-1} \tilde{M}^{-1} \right\|_\infty \leq \gamma \tag{18}$$

if $\gamma > 1$ and if and only if there is a symmetric matrix $R = R^T > 0$ that solves the following conditions:

$$(A + LC)R + R(A + LC)^T < 0 \tag{19}$$

$$\begin{pmatrix} AR + RA^T - \gamma BB^T & \bullet & \bullet \\ CR - \gamma DB^T & -\gamma E & \bullet \\ -E^{1/2}L^T & E^{1/2} & -\gamma I_p \end{pmatrix} < 0. \tag{20}$$

3.1 Static $\mathcal{H}_\infty$ loop shaping controller synthesis

Solving the sufficient LMI conditions (19)-(20) to determine the Lyapunov matrix $R = R^T > 0$, it is possible to obtain a static $\mathcal{H}_\infty$ controller that satisfies (18). From the control law $u = -Ky$, the realization of the closed-loop system is given by

$$T_{zw} = \left[\begin{array}{c|c} A_{MF} & B_{MF} \\ \hline C_{MF} & D_{MF} \end{array}\right] = \left[\begin{array}{c|c} A + B\tilde{K}C & (B\tilde{K} - L)E^{1/2} \\ \hline \tilde{K}C & \tilde{K}E^{1/2} \\ (C + D\tilde{K}C) & (I + D\tilde{K})E^{1/2} \end{array}\right] \tag{21}$$

where $\tilde{K} = -K(I + DK)^{-1}$.

Applying the *Bounded Real Lemma* (Scherer *et al.*, 1997; Boyd *et al.*, 1994) for the closed-loop system T_{zw} in order to achieve the $\mathcal{H}_\infty$-norm, we have

$$\Omega := \begin{pmatrix} A_{MF}R + RA_{MF}^T & RC_{MF}^T & B_{MF} \\ C_{MF}R & -\gamma I & D_{MF} \\ B_{MF}^T & D_{MF}^T & -\gamma I \end{pmatrix} < 0. \tag{22}$$

Analogously,

$$\Omega = \tilde{A} + \tilde{B}\tilde{K}\tilde{C} + \tilde{C}^T\tilde{K}^T\tilde{B}^T < 0. \tag{23}$$

with,

$$\tilde{A} = \begin{pmatrix} AR + RA^T & \bullet & \bullet & \bullet \\ 0 & -\gamma I_m & \bullet & \bullet \\ CR & 0 & -\gamma I_p & \bullet \\ -E^{1/2}L^T & 0 & E^{1/2} & -\gamma I_p \end{pmatrix}, \tag{24}$$

$$\tilde{B} = \begin{pmatrix} B \\ I_m \\ D \\ 0 \end{pmatrix}, \quad \tilde{C} = \begin{pmatrix} CR & 0 & 0 & E^{1/2} \end{pmatrix}. \tag{25}$$

Finally, the static $\mathcal{H}_\infty$ loop shaping controller is given by condition (23) and making $K = -\tilde{K}(I + D\tilde{K})^{-1}$.

4. CONTROL DESIGN AND EXPERIMENTAL RESULTS

There are studies and norms that define acceptable limits for vertical acceleration. The norm BS 6841 ISO 6808 and ISO 2631 quantifies ranges of acceleration to provide comfort (Oliveira *et al.*, 2014b). The Tab. 2 shows these values. It is important to mention that the laboratory plant used represents only a quarter-car model and other factors are not being considered. Moreover, the constraints of Tab. 2 demonstrate the perception of the acceleration by a person.

Table 2. Discomfort Scale - Norm BS6841. adapted from (Oliveira, 2014b).

Aceleration $[m/s^2]$	**Scale**
≤ 0.315	Comfortable
0.315 a 0.63	Slightly comfortable
0.5 a 1.0	Little comfortable Conf.
0.8 a 1.6	Uncomfortable
1.25 a 2.5	Very uncomfortable
> 2.5	Extremely uncomfortable.

Following the $\mathcal{H}_\infty$ loop shaping design procedure, the choice of the compensators herein was based on trial and error in order to obtain a good trade-off between performance and stability. In this case, it was addressed that the pre- and post-compensators are given by:

$$W_1 = 3.8067 \text{ and } W_2 = 1. \tag{26}$$

Now, solving the sufficient LMI conditions (19) and (20), a robustness margin of $\gamma = 4.0 (\varepsilon = 25\%)$ was found. This means an upper bound for nonparametric uncertainties of 25% for the active suspension's nominal model. In addition, the $R = R^T > 0$ matrix obtained was:

$$R = \begin{pmatrix} 1.9663 & -0.3525 & -1.2229 & 0.0445 \\ -0.3525 & 5.0995 & -0.1429 & -2.4446 \\ -1.2229 & -0.1429 & 2.4239 & -0.1544 \\ 0.0445 & -2.4446 & -0.1544 & 2.8319 \end{pmatrix}. \tag{27}$$

Replacing this result in (23), we can determine the static $\mathcal{H}_\infty$ controller $K = 0.1440$. Hence, it is possible to obtain the controller for implementation doing

$$K_c = W_2 K W_1 = 0.5482. \tag{28}$$

In order to demonstrate the effectiveness of the method, the nominal mass of $M_s = 2.45[kg]$ (2 discs) was varied for 1 disc ($M_s = 1.95[kg]$) and without any disk ($M_s = 1.45[kg]$). Such variations in the system can be seen in Fig. 5.

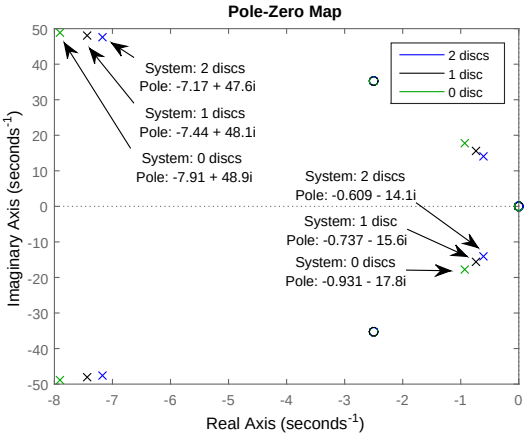

Figure 5. Influence of M_s in the active suspension's nominal model.

Moreover, a disturbance of $2[cm]$ in the road surface was applied for three experimental scenarios. The first scenario evaluates the performance of the static $\mathcal{H}_\infty$ controller found for the active suspension system having two disks. In Fig. 6a, it can be seen that acceleration decreased in amplitude and frequency. Such result provides greater comfort, when compared with the performance in open-loop.

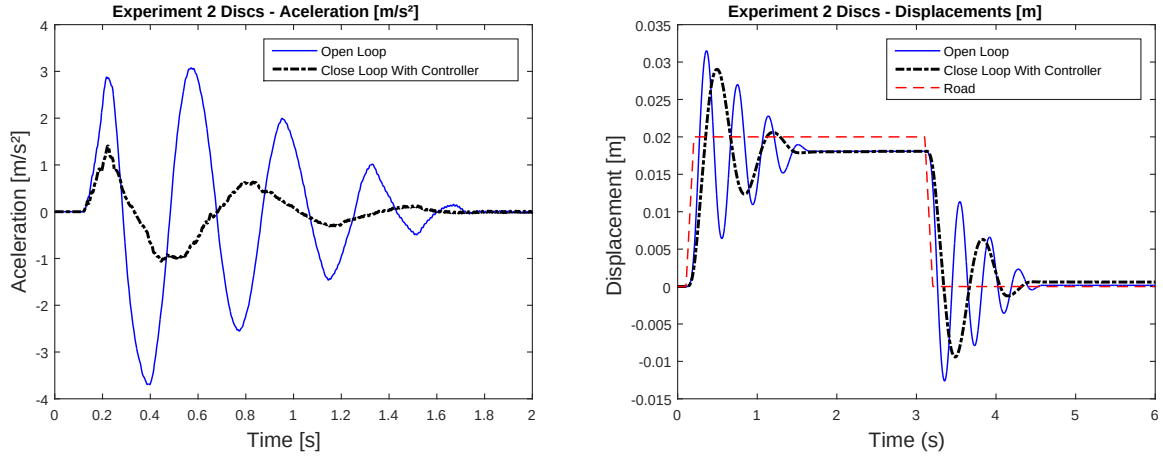

Figure 6. a) Comparison between open- and close-loop system for 2 discs; b) Registered displacements- 2 discs.

In Fig. 6b, the presence of a stationary error of the vehicle body and the road is presented. Such stationary error is justified by the dry friction that manifests intensely in the permanent regime. For the second scenario, the same experiment was performed for the active suspension system adopting only 1 disc. The Fig. 7 shows the results. Again, an attenuation of the maximum value of the acceleration and its oscillation is achieved.

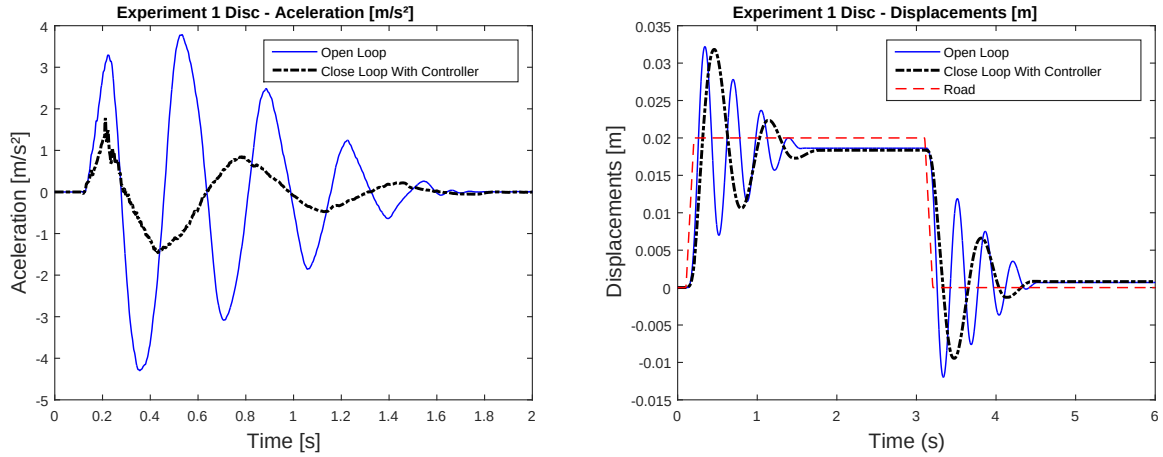

Figure 7. a) Comparison between open- and close-loop system for 1 discs; b) Registered displacements- 1 discs.

Finally, applying the same disturbance in the system with 0 disc (Fig. 8). The same results was achieved.

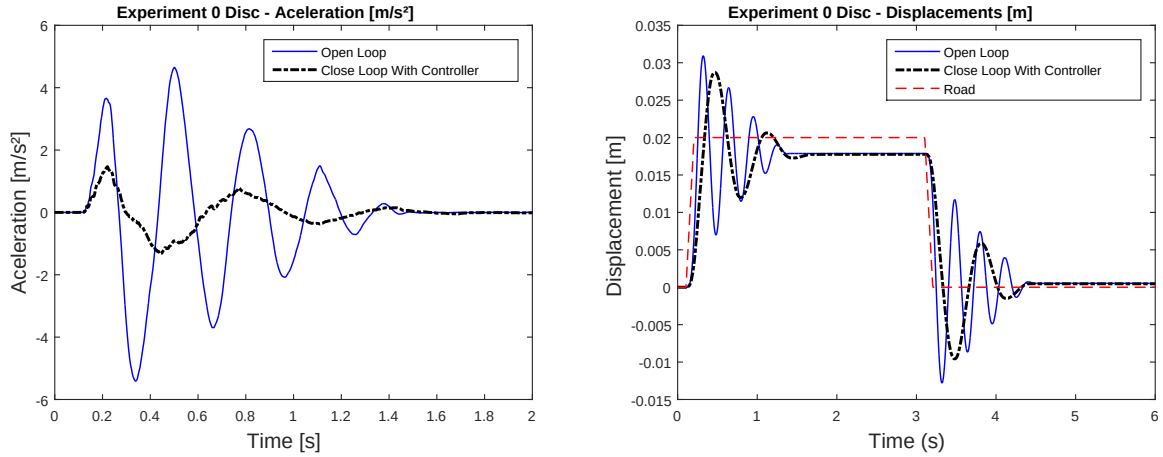

Figure 8. a) Comparison between open- and close-loop system for 0 discs; b) Registered displacements- 0 discs.

The maximum value of the acceleration of each experiment is compared with the open-loop system in Tab. 3 . It

is possible to observe a significant reduction in all cases. Even with variations in the model, the static $\mathcal{H}_\infty$ controller designed satisfies the requirements established.

Table 3. Maximum acceleration $[m/s^2]$.

Discs	Open-loop system	Close-loop system
0	5.409	1.467
1	4.297	1.781
2	3.691	1.408

In addition, bounders between $1.2A$ and $-1.2A$ were set for the control effort. The Fig. 9 shows that all the control signals respected the constraints.

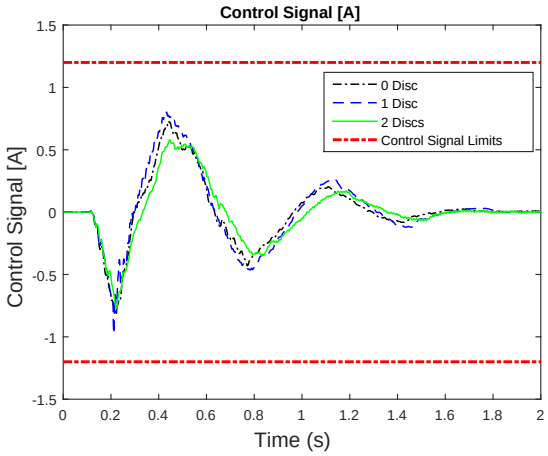

Figure 9. Control signals

5. CONCLUSION

In this paper, a practical implementation of a static $\mathcal{H}_\infty$ loop shaping controller applied in an active suspension system manufactured by Quanser Consulting was presented. The goal of the control design consists in showing that from just a static $\mathcal{H}_\infty$ gain, it was possible to obtain a robust performance and stability for the control of an active suspension system. Beside all the variations that the system allows, the static $\mathcal{H}_\infty$ controller designed presented an advantageous alternative to improve the active suspension performance. It attenuated the acceleration of the vehicle body and minimized the oscillations. Moreover, during all the experiments, the control effort remained on the limits defined previously preserving the equipment integrity and reliability. Finally, the experimental results obtained show that the static $\mathcal{H}_\infty$ loop shaping controller can be useful for the control of mechanical systems described by proper transfer function.

6. ACKNOWLEDGEMENTS

The authors acknowledge support provided by FAPEMIG.

7. REFERENCES

Alves, U.N.L.T., Garcia, J.P.F., Apolinario, G.C., Fernandes, U.B. and Rodrigues, F.B., 2013. "Controle de sistema de suspensão ativa por computador: Estratégia de controle robusto considerando atraso na aquisição de dados." *Simpósio Brasileiro de Automação Inteligente*.

Boyd, S., Ghaoui, L.E., Feron, E. and Balakrishnan, 1994. "Linear matrix inequalities in system and control theory." *SIAM Studies in Applied Mathematics*.

Fazzolari, H.A., Oliveira, P.C., Lordelo, A.D.S., Silva, E.R.P., Garcia, J.P.F., Teixeira, M.C.M. and ao, E.A., 2014. "Projeto de controle com estrutura variável e modos deslizantes de ordem completa por $\mathcal{D}$-estabilidade." *Congresso Brasileiro de Automática*.

McFarlane, D. and Glover, K., 1992. "A loop shaping design procedure using synthesis." *IEEE Transactions on Automatic Control*, Vol. 37, pp. 759–769.

Oliveira, D.R., Teixeira, M.C.M., ao, E.A., Souza, W.A., Moreira, M.R. and Silva, J.H.P., 2014a. "Projeto de controle robusto $\mathcal{H}_\infty$ chaveado: Implementação prática em um sistema de suspensão ativa." *Congresso Brasileiro de Automática*.

Oliveira, T.G., Dusse, A.C.S., Gonçalves, E.N. and aes, G.R.G., 2014b. "Controle $\mathcal{H}_\infty$ multiobjetivo de uma suspensão ativa." *Congresso Brasileiro de Automática*.

Pereira, R.L., Guaracy, F.H., Paula, C.F. and Pugliese, L.F., 2017a. "Controle $\mathcal{H}_\infty$ com formatação de malha a tempo discreto aplicado em um sistema de suspensão ativa." *Simpósio Brasileiro de Automação*.

Prempain, E. and Postlethwaite, I., 2005. "Static $\mathcal{H}_\infty$ loop shaping control of a fly-by-wire helicopter." *Automatica*, Vol. 41, pp. 1517–1528.

Quanser, 2013. "Laboratory guide: Active suspension experiment for matlab/simulink." *Ontario: [s.n]*.

Scherer, C., Gahinet, P. and Chilali, M., 1997. "Multi-objective output-feedback control via LMI optimization." *IEEE Transactions on Automatic Control*, Vol. 30, pp. 1307–1317.

Silva, E.R.P., Fazzolari, H.A., Oliveira, P.C., ao, E.A., Teixeira, M.C.M. and Lordelo, A.D.S., 2013. "Implementação prática da $\mathcal{D}$-estabilidade robusta via realimentação derivativa em um sistema de suspensão ativa." *Congresso Brasileiro de Automátical*.

8. RESPONSIBILITY NOTICE

The authors are the only responsible for the printed material included in this paper.